Extended Abstracts of the 16th (1984 International) Conference on Solid State Devices and Materials, Kobe, 1984, pp. 27-30

A-2-4

Fine Pattern Difinition with Focused Ion Beams and Its Application to X-Ray Mask Fabrication

Toshihiko KANAYAMA, Masanori KOMURO, Hiroshi HIROSHIMA,
Tsunehiro OHIRA, Nobufumi ATODA, Hisao TANOUE and Toshio TSURUSHIMA
Electrotechnical Laboratory
1-1-4 Umezono, Sakura-mura, Niihari-gun, Ibaraki 305, Japan

A new pattern definition method using atomic intermixing induced by focused-ion-beams (FIBs) is proposed; the intermixed region produced by FIB irradiation in the Al/Au system has a higher sputtering yield than Al and is selectively etched by a low-energy ion shower. With this method, X-ray masks were fabricated. Sub-quarter-micron patterns with high aspect-ratio were replicated from the fabricated mask in 1-μm thick PMMA layers with synchrotron radiation from the electron storage ring.

§1. Introduction

A micro-focused ion beam (FIB) obtained from a liquid-metal ion source is now expected to be used as a new tool for micro-fabrication. Generation of mask patterns for X-ray lithography is one of the most important uses of FIBs because X-ray lithography combined with FIBs is a promising candidate for sub-half-micron lithography.

For this mask fabrication, patterning of X-ray-absorber layers such as Au films is necessary. However, direct sputtering of the metal film by the FIB requires very high ion-dose; conventional photo or electron-beam resists are not adequate for heavy-ion exposure because their sensitivity to the heavy ion is so high that the exposed pattern is affected by the statistical fluctuation of the intensity within a beam and because the range of the heavy ion is too small to a resist with a desirable thickness.

In this paper, we propose a new method of pattern definition in Au films with FIB exposure followed by ion milling. With this method, X-ray lithography masks with a-quarter-micron patterns have been fabricated. Pattern transfer characterictis of the fabricated mask with synchrotron radiation is also discussed.

§2. Pattern Definition Method

The pattern definition process proposed here is shown in Fig. 1. The sample consists of double layers of Al and Au. First, a thin Al layer on the top is intermixed with the underlying Au layer by irradiation with the FIB. This intermixed Au-Al region has a higher sputtering rate than Al; hence ion milling over the entire surface after the FIB exposure engraves the Au layer only at the position exposed to the FIB with the un-exposed Al as an etching mask. The ion beam used for the milling does not cause the intermixing because its energy, generally much lower than that of the FIB, is too small for the ion to reach the Al/Au interface and to cause the intermixing.

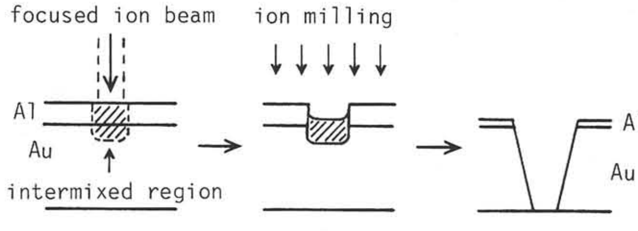

Fig. 1. The pattern definition process proposed in the text.

The reason why the intermixed Au-Al has a larger sputtering yield than Al is principally as follows. According to Sigmund[1], the sputtering yield is proportional to the energy deposition of the incident ion at the surface and inversely proportional to the binding energy of the atom to the surface. Aluminum has a smaller energy deposition and therefore has a smaller sputtering yield than Au. The intermixed Au atoms into the Al layer increase the energy deposition without largely changing the binding energy and consequently enhance the sputtering yield of the Al atom.

In the present work, ion milling was performed with 4-keV Xe ions in an O_2 ambient of $5x10^{-3}$ Pa. By adopting an extremely heavy ion like Xe, the difference in the sputtering yield between Al and Au is magnified by increasing the difference in the energy deposition. Addition of O_2 during ion milling is very efficient to suppress the sputtering yield of Al; the sputtering yield of Au is not affected by the presence of O_2. The sputtering rate ratio of Au:Au_5Al_2:Al was measured to be about 30:6:1 in the sputtering condition mentioned above and 7:4:1 unless O_2 was added (in the latter case, the partial pressure of O_2 was less than 10^{-4} Pa).

The exposure characteristics of a 16-nm Al/ 195-nm Au sample to 50-keV Ga^+ beams are shown in Fig. 2. Figures besides the curves indicate the dose of Xe ions used for the etching. In Fig. 2, it is clearly observed that the Ga^+ exposure enhances the etch depth in Xe-ion milling; the depth etched by the Xe ions following the Ga^+ exposure is much larger than that calculated from the sputtering yield of Al and Au by the Ga^+ and the Xe ion beams. It is interesting to note in Fig. 2 that the depth sputter-etched with the Ga^+ beam itself in the Al/Au sample is also larger than that in Al without an underlying Au layer. We believe this enhancement in the etch depth results from the intermixing between Al and Au induced by Ga^+ bombardment.

As shown in Fig. 2, the Ga^+ exposure dose of $6x10^{15}$ ions/cm^2 is sufficient to define patterns in this 0.2-µm-Au sample. It should be noted that this dose is considerably smaller than both that required for etching directly the Au layer (the required dose is about $8x10^{16}$ ions/cm^2 for 0.2-µm Au) and that required for sputtering off the 16-nm Al layer ($4x10^{16}$ ions/cm^2 as shown in Fig. 2).

In order to confirm that the ion bombardment actually produces intermixing in the Al/Au system, X-ray diffraction was measured with a Seeman-Bohlin type diffractometer with an incidence angle of 2°. Figure 3 (b) shows an X-ray diffraction pattern for a 20-nm Al/ 0.2-µm Au sample bombarded with 100 keV Kr^+ ions at room temperature to a dose of $5x10^{15}/cm^2$. Compared with Fig. 3 (a),

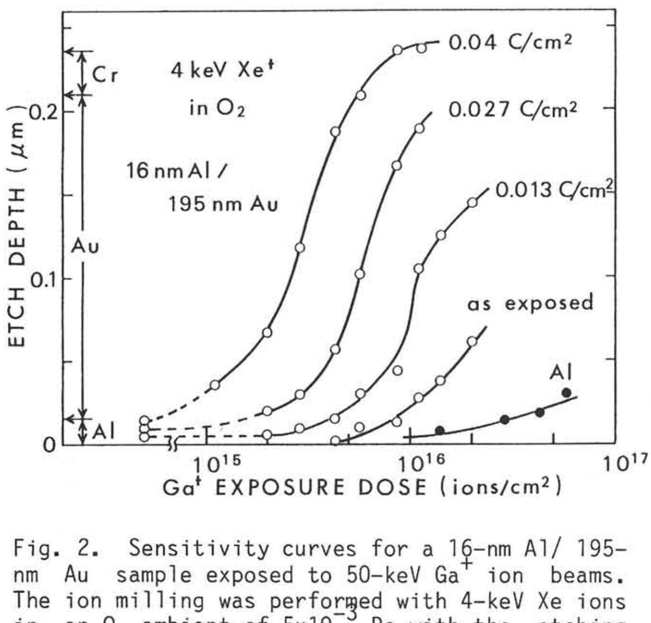

Fig. 2. Sensitivity curves for a 16-nm Al/ 195-nm Au sample exposed to 50-keV Ga^+ ion beams. The ion milling was performed with 4-keV Xe ions in an O_2 ambient of $5x10^{-3}$ Pa with the etching dose indicated. A thin Cr layer was used as a glue layer between the Au layer and the Si substrate. Closed circles indicate the depth sputter-etched by 50-keV Ga^+ ions in a thick Al layer without an underlying Au layer.

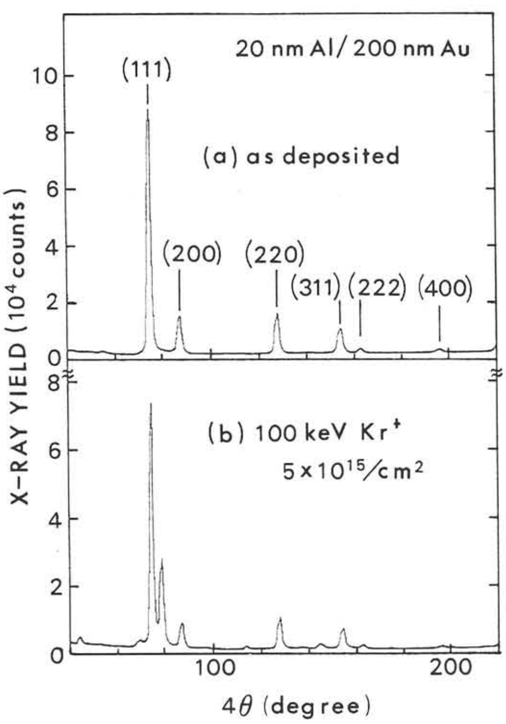

Fig. 3. Glancing-incidence X-ray diffraction patterns for 20-nm Al/ 0.2-µm Au samples as-deposited (a) and bombarded with 100-keV Kr^+ ions to a dose of $5x10^{15}/cm^2$ (b). In (a), all the peaks are identified as diffraction peaks from Al and Au; diffraction indices are shown in the figure (Al and Au have nearly equal lattice constants).

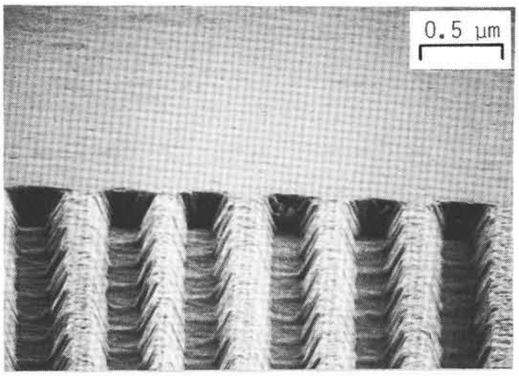

18 nm Al / 203 nm Au
5.2×10^{-8} C/cm, 0.06 C/cm^2

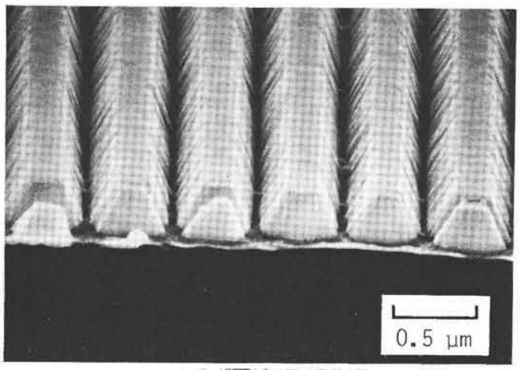

22 nm Al / 290 nm Au
7.8×10^{-8} C/cm, 0.05 C/cm^2

Fig. 4. SEM micrographs of the grooves fabricated with 50-keV Ga^+ beams with a diameter of 0.2 μm. The viewing angle is 80°. The sample structure, the line dose of the Ga^+ beam and the etching dose of the 4-keV Xe ions are indicated below each micrograph.

several excess peaks besides those of Al and Au appear in Fig. 3 (b) to indicate that some new phase was formed after the ion bombardment. We believe this new phase has resulted from the intermixing between Al and Au, although we have not yet identified the phase formed.

Figure 4 shows SEM micrographs of the grooves formed in Au layers. For groove fabrication, line exposures to micro-focused 50-keV Ga^+ ion beams with a diameter of 0.2 μm in F.W.H.M. were performed in a focusing column reported previously[2] (the diameter of the beam used was estimated by observing the width of the grooves formed with ion-bombardment-enhanced etching method in Si and GaAs[3]). In Fig. 4, grooves with a width less than a quarter micron are successfully formed.

However, the slope of the groove wall is not vertical but has a constant value of about 70°. Owing to this, the aspect ratio obtainable with the present patterning process is limited to about unity. Moreover, prolonged etching with Xe ions was observed to produce widening of the groove.

These observations suggest that the Xe ions also cause intermixing at the Al/Au interface revealed at the groove wall and produce side etching; thus, the slope of the groove wall is determined by the dependence of the sputtering yield on the incidence angle of the ion beam to the sample surface. Therefore, we believe that improvement in the pattern shape can be achieved by employing better etching process than purely physical sputter etching.

§3. Fabrication of X-Ray Masks

The fabrication procedure of X-ray lithography masks is presented in Fig. 5. First, a SiO_xN_y film, which acts as a supporting membrane is deposited by plasma-CVD on a (100) Si substrate. Next, this Si substrate is etched from the backside in hot KOH solution and mask windows are formed. Then, Al, Au and Al films are successively deposited on the SiO_xN_y. The bottom Al layer serves as an etching stop and also as glue between the Au layer and the SiO_xN_y. Finally, the sample is irradiated with a FIB and the Au layer is patterned with the method mentioned above.

Figure 6 shows SEM photographs of the fabricated mask and the patterns transferred to PMMA (poly-methyl-methacrylate) from this mask with synchrotron radiation. The supporting membrane of the mask is a 1-μm thick composite $SiO_2/SiO_xN_y/SiO_2$ film and the metalization consists of 21-nm Al/ 320-nm Au/ 27.5-nm Al. Pattern definition in the Au layer was carried out by irradiating with focused 50-keV Ga^+ beams with a diameter of 0.2 μm in F.W.H.M. to a dose of 7.8×10^{-8} C/cm followed by etching with 4-keV Xe ions to a dose of 0.06

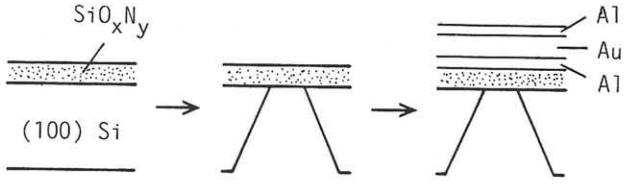

Fig. 5. Fabrication procedure of X-ray lithography masks.

C/cm^2. For pattern replication, Si wafers coated with PMMA were placed in contact with the mask and exposed to synchrotron radiation obtained from the electron storage ring at Electrotechnical Laboratory[4,5]. The energy of the stored electrons was 600 MeV; the intensity of the radiation is strongest at a wave length of 1.8 nm. The exposure dose is indicated in Fig. 6 in terms of stored-electron current multiplied by exposure time. The exposed resist was developed in methyl-isobutyl-ketone (MIBK) at 20°C.

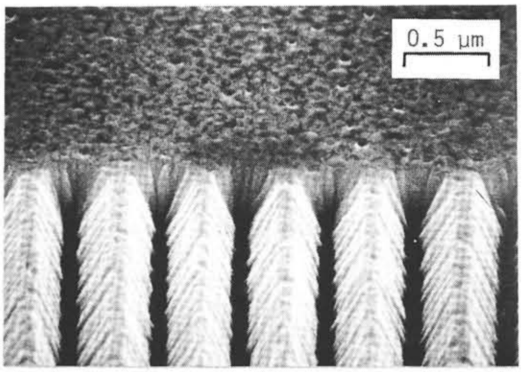

(a) structure: 21 nm Al/ 320 nm Au/ 27.5 nm Al (top) (bottom)
Ga^+ dose: 7.8×10^{-8} C/cm, Xe^+ dose 0.06 C/cm^2

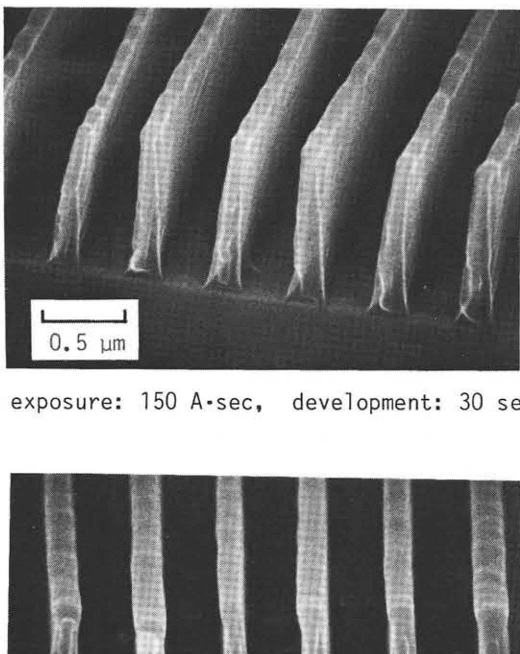

(b) exposure: 150 A·sec, development: 30 sec

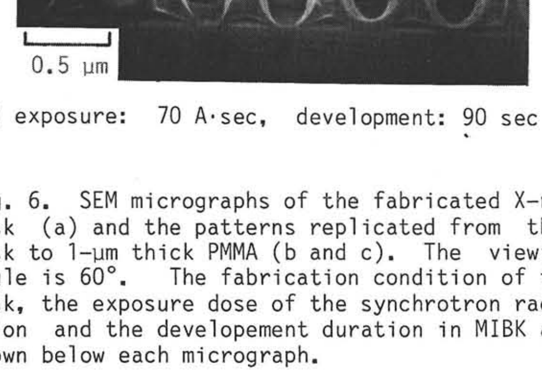

(c) exposure: 70 A·sec, development: 90 sec

Fig. 6. SEM micrographs of the fabricated X-ray mask (a) and the patterns replicated from this mask to 1-μm thick PMMA (b and c). The viewing angle is 60°. The fabrication condition of the mask, the exposure dose of the synchrotron radiation and the developement duration in MIBK are shown below each micrograph.

In Fig. 6 (b), very sharp lines with a width less than 0.2 μm are drawn in 1-μm thick PMMA (bending in the line pattern was caused by heating during SEM observation). However, the line wall is not vertical and is slightly round in the bottom, reflecting the shape of the mask absorber. This shortcoming is emphasized when the exposure is under as shown in Fig. 6 (c). In Fig. 6 (c), the line is connected at some places across the grooves. For formation of steep patterns with high aspect ratio, precise control of exposure dose is required.

§4. Summary

We have proposed a new pattern definition method utilizing enhancement in sputtering yield resulting from FIB-induced intermixing in the Al/Au system. This method was applied to the fabrication of X-ray lithography masks. From the fabricated mask, steep patterns narrower than 0.2 μm were successfully replicated into 1-μm thick PMMA using synchrotron radiation obtained from the electron storage ring.

Acknowledgement

We would like to thank Drs. T. Tomimasu, K. Hoh and M. Hirata and the staffs of High Energy Radiation Section of Electrotechnical Laboratory for the operation of the storage ring and the synchrotron-radiation lithography facilities.

References

1) P. Sigmund: Phys. Rev. 184 (1969) 383.
2) M. Komuro: Thin Solid Films 92 (1982) 155.
3) M. Komuro, T. Kanayama, H. Hiroshima, and H. Tanoue: Appl. Phys. Lett. 42 (1983) 908.
4) T. Tomimasu, T. Noguchi, S. Sugiyama, T. Yamazaki, T. Mikado, and M. Chiwaki: IEEE Trans. Nucl. Sci. NS-30 (1983) 3133.
5) K. Hoh, M. Hirata, N. Atoda, H. Tanino, S. Ichimura, and H. Onuki: Jpn. J. Appl. Phys. 22 (1983) Suppl. 22-1, p.661.